



OPEN

Visualizing structural dynamics of thylakoid membranes

SUBJECT AREAS:

PHOTOSYNTHESIS

3-D RECONSTRUCTION

Masakazu Iwai^{1,2}, Makio Yokono³ & Akihiko Nakano^{1,4}Received
2 August 2013Accepted
27 December 2013Published
20 January 2014Correspondence and
requests for materials
should be addressed to
M.I. (miwai@riken.jp)

¹Live Cell Molecular Imaging Research Team, Extreme Photonics Research Group, RIKEN Center for Advanced Photonics, 2-1 Hirose, Wako, Saitama 351-0198, Japan, ²PRESTO, Japan Science and Technology Agency (JST), Honcho, Kawaguchi, Saitama 332-0012 Japan, ³Institute of Low Temperature Science, Hokkaido University, Sapporo, Hokkaido 060-0819 Japan, ⁴Department of Biological Sciences, Graduate School of Science, The University of Tokyo, Bunkyo-ku, Tokyo 113-0033, Japan.

To optimize photosynthesis, light-harvesting antenna proteins regulate light energy dissipation and redistribution in chloroplast thylakoid membranes, which involve dynamic protein reorganization of photosystems I and II. However, direct evidence for such protein reorganization has not been visualized in live cells. Here we demonstrate structural dynamics of thylakoid membranes by live cell imaging in combination with deconvolution. We observed chlorophyll fluorescence in the antibiotics-induced macrochloroplast in the moss *Physcomitrella patens*. The three-dimensional reconstruction uncovered the fine thylakoid membrane structure in live cells. The time-lapse imaging shows that the entire thylakoid membrane network is structurally stable, but the individual thylakoid membrane structure is flexible *in vivo*. Our observation indicates that grana serve as a framework to maintain structural integrity of the entire thylakoid membrane network. Both the structural stability and flexibility of thylakoid membranes would be essential for dynamic protein reorganization under fluctuating light environments.

Photosynthetic organisms have developed flexible machinery for effective light energy use^{1,2}. To increase the light energy absorption in photosystem II (PSII), the association of light-harvesting antenna complex II (LHCII) with PSII is induced in chloroplast thylakoid membranes, forming the PSII-LHCII supercomplex³. The rate of light energy absorption in photosystem I (PSI) is reversibly raised by the dissociation of LHCII from PSII^{4,5} and also the association of LHCII with PSI⁶⁻⁸. In green algae, the association of LHCII with PSI not only increases PSI excitation^{9,10} but also causes the interaction of cytochrome *b₆f* complex with PSI¹¹, leading to the switch from linear electron transport to cyclic electron transport around PSI^{12,13}. In higher plants, cyclic electron transport is stimulated by the association of chloroplast NADH dehydrogenase-like complex with PSI¹⁴. Moreover, the reorganization of PSII-LHCII supercomplex is essential for energy dissipation mechanism under intense light conditions to protect PSII from excess energy¹⁵⁻¹⁷, in which the protein interactions with LHCSR3 and PSBS are involved in green algae and higher plants, respectively^{18,19}. When PSII is damaged, disassembly of PSII occurs after its migration from the stacked, appressed membranes, or grana, to the single-layer, stroma-exposed membranes, or stroma lamellae, where PSII subunits are replaced^{20,21}. Based on these facts, the structure and arrangement of thylakoid membranes have to be flexible for such protein reorganization to be taken place in response to changing light environments.

The structure and arrangement of thylakoid membranes have long been studied since the first observation using light microscopy by Hugo von Mohl in 1837. The grana inside chloroplasts are already identified by light microscopy as dense, dot-like structures²². Introducing electron microscopy has deepened our understanding of the structural complexity of thylakoid membranes, showing the remarkable architecture in which stroma lamellae connect to grana in the helical configuration²³⁻²⁶. Recently, electron tomography has determined the three-dimensional (3D) structure of thylakoid membranes in higher plants^{27,28}, revealing the distinctive image of the junctional connections between grana and stroma lamellae. Intriguingly, the junctional slits where stroma lamellae connect grana show significant structural variations^{27,28}, reflecting the variability of the membrane structure. Although electron tomography provides a comprehensive picture of thylakoid membrane structure with ~1 nm resolution, it cannot determine the spatiotemporal dynamics. Therefore, to demonstrate the dynamic aspect of thylakoid membrane structure *in vivo*, the visualization by live cell imaging is essential.

In this work, we used conventional confocal microscopy to observe chlorophyll (Chl) fluorescence structures inside chloroplasts. Previous studies have already shown Chl fluorescence images of chloroplasts in various green algae and higher plants^{29,30}. Although confocal microscopy exhibits Chl fluorescence structure in live cells, the fine membrane structure is hardly visible by conventional confocal microscopy due to the diffraction limited



resolution³¹. Also, autofluorescence from numerous Chl pigments in thylakoid membrane proteins causes too much signal to resolve the fine membrane structure. In addition, chloroplasts are normally 5 ~ 10 μm in size, which makes difficult to discern the inside membrane structure. To overcome these problems, we used the moss *Physcomitrella patens* protonemata to observe the membrane structure in the macrochloroplast, which is more than 10 times larger than normal chloroplasts^{32,33}, and applied 3D deconvolution to the serial optical sections of confocal images^{34,35}. We also performed 3D time-lapse imaging to determine the spatiotemporal dynamics of thylakoid membrane structure. Our observation suggests that thylakoid membranes contain significantly flexible structures *in vivo*. The dynamic aspect of thylakoid membrane structure in relation to the photoacclimation mechanisms will be discussed.

Results

The reconstructed 3D image of thylakoid membrane structure in the *P. patens* macrochloroplast. To visualize thylakoid membrane structure inside chloroplasts, we used the moss *P. patens* protonemata, which usually contain ~50 chloroplasts in each cell (Fig. 1a). Although confocal microscopy techniques have improved image quality, the optical aberrations and the out-of-focus blur will easily lower the actual resolution under the theoretical limit, especially using complicated biological samples. In case of chloroplasts, numerous Chls exist in photosynthetic proteins in thylakoid membranes, so the internal membrane structure is merely visible because of too much Chl fluorescence signal (Fig. 1b). To increase the image contrast and to decrease the effect of out-of-focus signals, we performed 3D deconvolution³⁵. The reconstructed 3D image showed that the blurred Chl signals were significantly reduced, revealing the Chl fluorescence structures inside the chloroplasts (Figs. 1c, d). Since Chl pigments present in thylakoid membrane proteins, the structure shown by Chl fluorescence indicated solely thylakoid membranes. But, it was still difficult to analyze thylakoid membrane structure because of the ~10 μm size of chloroplasts and their random movement during the observation. Interestingly, *P. patens* chloroplast division is involved with peptidoglycan synthesis³². We thus treated the protonemata with ampicillin to inhibit peptidoglycan synthesis, leading to the macrochloroplast formation in each cell (Figs. 1e, f). Previous studies have confirmed no difference in the shape and size of thylakoid membrane structure between normal chloroplasts and macrochloroplasts as examined by electron

microscopy^{32,33}. We then applied 3D deconvolution to the observed serial sections of Chl fluorescence confocal images. The reconstructed 3D image demonstrated the more detailed thylakoid membrane network inside the macrochloroplast (Figs. 1g, h). Within the membrane network, there were two distinct structures—the dot-like and thread-like structures (Fig. 1i, arrows and arrow heads, respectively). Comparing the images before and after 3D deconvolution indicated that the reconstructed 3D image does not generate any unnatural structures but effectively diminishes the out-of-focus blur of Chl fluorescence (Fig. S1). The average diameter of the dot-like structures was 425 ± 70 nm ($n = 25$; Fig. S2), which is equivalent to the size of grana as suggested previously³⁶. Thus, the dot-like structures most likely represent grana.

Structural stability and flexibility of thylakoid membranes. We next performed 3D time-lapse imaging of *P. patens* macrochloroplasts. The time resolution of our confocal microscopy setup was ~1.3 s per slice, taking ~7 s to obtain each 3D image, so we could not resolve the fast movement occurring within ~7 s intervals. The reconstructed 3D time-lapse images demonstrated the dynamic movements of thylakoid membrane structure (Fig. 2a and Supplementary Movie 1). The entire thylakoid membrane network was not stable but rather showing random oscillations. Interestingly, the location of the dot-like structures was almost stationary during the observation (Figs. 2b, c). This also suggests that the dot-like structures represent grana. The sum image of the 28 observed Chl fluorescence images during the observation also showed that the structural patterns were mostly comparable to that of the initial image (Fig. 2d). This implies that the entire thylakoid membrane network is not largely rearranged during the observation.

As compared to the dot-like structures, the thread-like structures showed more dynamic movement. The spatial arrangement of the thread-like structures changed within the 7 s intervals during the 3D time-lapse imaging (Fig. 3a). It was evident that the thread-like structures stretched out from a dot-like structure to the neighboring structures. Although the location of the dot-like structures was mostly unchanged as described in Fig. 2, the dot shape looked flexible, being circular, ovate, and irregularly oblong (Fig. 3a, b). Moreover, 3D time-lapse imaging also demonstrated structural flexibility of the interconnection between the dot-like and thread-like structures (Fig. 3b). The thread-like structures were extended from at least four different locations around the dot-like structure. Since we observed Chl fluorescence, we could not determine whether such an

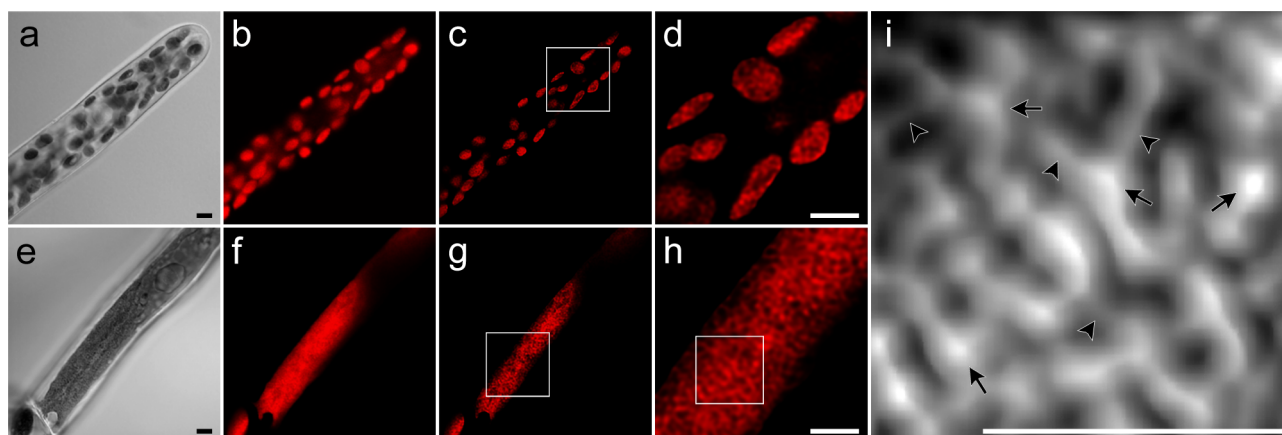


Figure 1 | Thylakoid membrane network revealed by confocal microscopy in combination with 3D deconvolution. (a–d) The normal chloroplasts in *P. patens* protonemata grown on the agar media in a glass-bottom dish were directly observed. (e–i) The formation of macrochloroplasts was induced by growing on the agar media containing 1 mM ampicillin in a glass-bottom dish. (a), (e) The differential interference contrast images. (b), (f) The chlorophyll fluorescence images. (c), (g) The reconstructed 3D images of chlorophyll fluorescence. (d), (h) The enlarged images of the squares in (c) and (g), respectively. (i) Surface plot after linear contrast adjustments of the enlarged image of the square in (h). The arrows and arrowheads indicate the dot-like and thread-like structures, respectively. Scale bars, 5 μm .

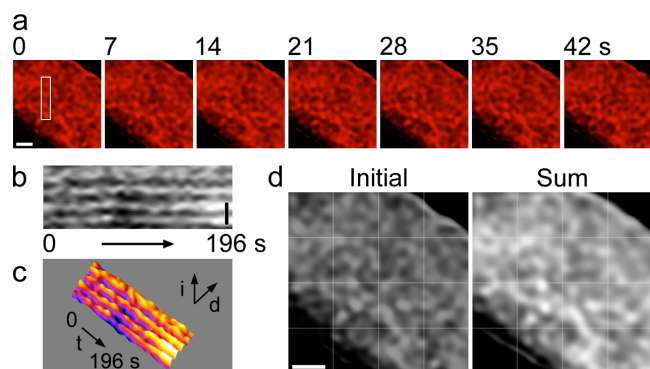


Figure 2 | The spatiotemporal dynamics of thylakoid membrane structure in the macrochloroplast under the control conditions. (a) The 3D time-lapse images of the *P. patens* macrochloroplast showed the random oscillation of thylakoid membrane structure (see also Supplementary Movie 1). Numbers indicate the elapsed time in seconds during the observation. (b) The kymograph of the square in (a) suggested that the location of the dot-like structures were mostly unchanged during the observation. (c) Surface plot of kymograph in (b). Arrows indicate the directions for fluorescence intensity (i), the distance (d), and the time (t). (d) The entire thylakoid membrane network of the initial image was almost the same as the sum image of the 28 recorded images during the observation for 196 s. Scale bars, 2 μm .

observed dynamic movement implies the movement of the membrane proteins or the membrane itself. Also, it is almost unavoidable that each 3D image contains different time axes between Z-planes, leading to the possible artifactual structures introduced by the 3D deconvolution in case of fast moving objects in live cell (see also Supplementary Note for the evaluation of the effect in our obtained results). Nevertheless, our 3D time-lapse imaging could distinguish the two structurally different objects inside the chloroplasts—the dot-like structures that are structurally stable at least 7 second and the thread-like structures that are not structurally stable as compared to the dot-like structures.

Enhanced structural flexibility of thylakoid membranes caused by the decreased number of PSII. Earlier studies have suggested that the subcompartmentalization of thylakoid membranes into grana and stroma lamellae largely depends on the localization of PSI and PSII^{37–40}. To examine whether the number of PSII affects the observed dot-like structures, we next treated the protonemata with lincomycin, which prevents chloroplast-encoded protein synthesis, thereby decreasing the number of PSII⁴¹ (Fig. S4). The reconstructed 3D image of the lincomycin-treated macrochloroplast still showed the thylakoid membrane network, but the dot-like structures appeared to be smaller (Fig. 4a). The average diameter of the dot-like structures was 310 ± 50 nm ($n = 25$; Fig. S2), about 27% smaller than the ones observed under the control conditions. The result suggested that the decreased number of PSII reduces the size of the dot-like structures, indicating again that the dot-like structures represent grana.

The 3D time-lapse imaging of the lincomycin-treated macrochloroplast indicated that most of the thylakoid membrane network showed dynamic movement (Fig. 4a and Supplementary Movie 2). It was apparent that the entire thylakoid membrane network moved more dynamically than the one observed under the control conditions. Because of the more dynamic movement and also the smaller size of the dot-like structures, the distinction between the two structures became less obvious. Moreover, the location of the dot-like structures became unstable, along with the dynamic movement of the thread-like structures (Figs. 4b, c). The movement of the thread-like structures was also not restricted to one particular location but

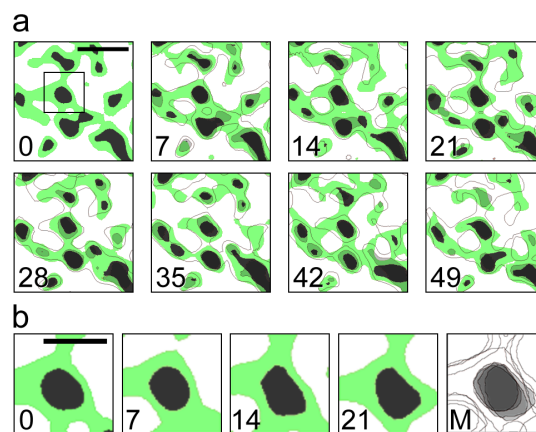


Figure 3 | Structural dynamics of the thread-like structures. (a) Chl fluorescence signal indicating the dot-like (black) and thread-like structures (transparent green) was extracted from Supplementary Movie 1. The structures observed in the previous panel are faintly outlined in the next panel to compare the structural changes between the sequential images. Numbers indicate the elapsed time in seconds during the observation. Scale bar, 2 μm . (b) The enlarged images of the square in (a) with the transparent green indicating the thread-like structures. M, the merged image, focusing on the structural variations of the dot-like structures (transparent grey) during the observation. Numbers indicate the elapsed time in seconds during the observation. Scale bar, 1 μm .

moving randomly in most of the chloroplast stromal space (Fig. 4d). These results suggest that the reduced number of PSII by lincomycin treatment makes the dot-like structures unstable so that the entire thylakoid membrane network becomes more randomly oscillated (Fig. 4e). Previous study shows that lincomycin treatment increases the amount of LHCII relative to that of PSII in thylakoid membranes⁴¹. Therefore, the enhanced structural dynamics of the thread-like structures was caused by the increased number of LHCII and/or the decreased number of PSII in the total thylakoid membranes.

Discussion

The extensive studies by using a variety of microscopy have determined the structural aspect of thylakoid membranes⁴². Also, the reversible structural modification that affects the gross multilamellar organization of thylakoid membranes has been demonstrated *in vivo*^{43,44}. However, the correlation between thylakoid membrane structure and its dynamic aspect has not been directly visualized in live cell. In this study, we visualized for the first time the spatiotemporal dynamics of thylakoid membrane structure by using live cell imaging technique. Our observation revealed the complex network of thylakoid membranes in the *P. patens* macrochloroplast, which consists of the dot-like structures interconnected by the thread-like structures (Fig. 1). The formation of macrochloroplasts in the *P. patens* protonemata is crucial for our live cell imaging. Because the normal chloroplasts continuously move around in the cytosol, it is almost impossible to differentiate whether the observed structural dynamics is caused by the actual thylakoid membrane dynamics or the chloroplast movement. Forming the macrochloroplast in the protonemal cell effectively prohibits the chloroplast movement since it becomes large enough to fill in the cytoplasm (Fig. 1e). Also, it has been verified that thylakoid membrane structure in the *P. patens* macrochloroplast is the same as in the normal chloroplast^{32,33}. Therefore, the macrochloroplast formation is essential for not only visualizing the detailed thylakoid membrane network but also confirming that our observation demonstrates the actual structural dynamics of thylakoid membranes *in vivo*.

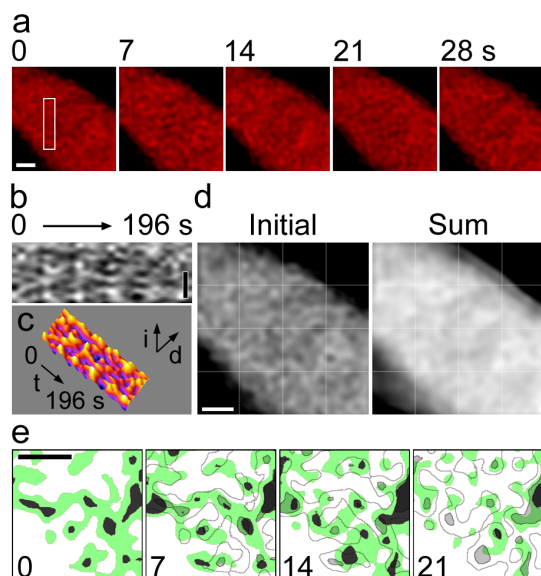


Figure 4 | The enhanced structural dynamics of thylakoid membranes in the lincomycin-treated macrochloroplast. (a) The 3D time-lapse imaging of the *P. patens* macrochloroplast treated with 1 mM lincomycin showed more dynamic movement of thylakoid membrane structure as compared to the control conditions (see also Supplementary Movie 2). Numbers indicate the elapsed time in seconds during the observation. (b) The kymograph of the square in (a) shows that the location of the dot-like structures was randomly changed during the observation. (c) Surface plot of kymograph in (b). Arrows indicate the directions for fluorescence intensity (i), the distance (d), and the time (t). (d) The entire thylakoid membrane network of the initial image became mostly vague in the sum image of the 28 recorded images during the observation for 196 s. (e) Chl fluorescence signal indicating the dot-like (black) and thread-like structures (transparent green) was extracted from Supplementary Movie 2. The structures observed in the previous panel were faintly outlined in the next panel to compare the structural changes between the sequential images as in Fig. 3a. Numbers indicate the elapsed time in seconds during the observation. Scale bars, 2 μm .

Our live cell imaging shows that the entire thylakoid membrane network is stable (Fig. 2). In particular, the location of the dot-like structure is mostly unchanged during the observation. The result is quite reasonable if we assume that the dot-like structures are grana, which are cylindrical stacks of tightly appressed membrane layers as shown by electron tomography^{27,28}. The similar observation has also been shown previously using fluorescence recovery after photo-bleaching technique⁴⁵. Interestingly, although the entire thylakoid membrane network is stable, the individual dot-like structure is not completely fixed as showing the random oscillations (Supplementary Movie 1). Besides, our observation indicates that the shape of the dot-like structure is variable in time (Fig. 3b). This implies that the dot-like structures are structurally stable but also flexible *in vivo*. These observations could indicate the unique feature of smectic mesophases of the biological membrane. Previously, the *in vitro* observation using atomic force microscopy has suggested such dynamic aspects of grana⁴⁶. There are certain mass-free spaces within PSII arrays in grana, indicating the presence of membrane domains where protein interaction and reorganization can occur. LHCII is also suggested to regulate the reorganization of the multibilayer architecture of grana upon its phosphorylation^{44,47}. Therefore, the membrane conditions of the dot-like structures, or grana, could be much more flexible than previously thought.

In addition, our observation revealed that the thread-like structures showed considerable structural flexibility *in vivo* (Fig. 3a). What the thread-like structures actually reflect is not yet certainly

determinable. Since our observation suggests that the dot-like structures most likely indicate grana, the thread-like structures, which interconnect the dot-like structures, reflect most likely stroma lamellae, where PSI is known to be abundant. However, PSI fluorescence is hardly visible at room temperature⁴⁸, so the observed Chl fluorescence of the thread-like structures is mostly originated from PSII and/or LHCII. There are two possibilities to describe the thread-like structures. First, the significant structural flexibility of the thread-like structures reflects the dynamic protein interactions involved with PSII and LHCII, which are known to be important processes to regulate photoacclimation mechanisms such as state transitions^{3–5} and energy dissipation mechanism^{15–19}. Thus, the apparent structural dynamics of the thread-like structures could be caused by the changes in Chl fluorescence lifetime due to the changes in the functional antenna size of PSII⁴⁹. Second, the observed thread-like structures represent free LHCII existing as a pool, which is suggested to be critical to readily redistribute the excitation energy to PSI in state transitions^{50,51}. In that case, the thread-like structures could indicate the grana margins, where PSI is known to be involved in state transitions⁵². As we observed the thread-like structures extending from the dot-like structures (Fig. 3a), it is possible that such LHCII pools are visible in the stroma lamellae particularly when there is no functional interaction with PSI. Therefore, the observed structural dynamics could be caused by the dynamic interactions of LHCII with PSI occurring in grana margins or stroma lamellae.

According to the lamellar phase characteristics of the membrane as described above, we cannot exclude the possibility that such structural dynamics reflects the fusion and fission of the membrane interacting with grana. Previously, the similar structural rearrangement has been suggested by the observation using de-enveloped chloroplasts⁵³. It is possible that such fusion and fission of the membranes may cause the transport of a large amount of proteins between neighboring grana. However, even if it is the case, we cannot visualize the process by our microscopy setup used in this study because such a membrane fusion occurs within a millisecond⁵⁴.

We observed that the thread-like structures stretched out from various locations of margins of the dot-like structures (Fig. 3b). Such structural variability could reflect the inter-grana membrane regions, which have been observed by earlier electron microscopy²⁴. Recent electron tomography has also confirmed the variable size of junctional connections between grana and stroma lamellae^{27,28}. Also, the reorganization of thylakoid membrane ultrastructure has been demonstrated *in vivo*^{55,56}. From these results, our observation implies that the structural variability shown by electron microscopy actually reflects structural flexibility of grana margins *in vivo* (Fig. 3b). Such structural flexibility could be essential because grana margins are suggested to be important regions for various regulatory processes^{53,57}. This observation can also be explained by the changes in Chl fluorescence lifetime and/or the possible fusion and fission process involving the thread-like structures as described above.

Moreover, our observation indicates the correlation between the dot-like structures and structural dynamics of the entire thylakoid membrane network. Previously, it has been shown that the number of LHCII affects the grana formation⁵⁸. Our result shows that the decrease in the number of PSII (Fig. S3) also influences the size of the dot-like structures, which most likely indicates the decrease in grana size (Fig. 4a and Fig. S2). These suggest that the formation of PSII-LHCII supercomplex is essential for the structural stability of grana with optimal size⁵⁹. As a matter of fact, our observation reveals that the decrease in the size of the dot-like structures enhances the dynamic movement of the entire thylakoid membrane network, especially the thread-like structures, moving much more randomly as compared to the control conditions (Fig. 4 and Supplementary Movie 2). One of the possibilities to explain such situations is that the observed structural dynamics indicates mostly PSII fluorescence, but because of the increased number of LHCII relative to that of PSII⁴¹



(Fig. S3), there should be some portions of LHCII, which are not connected with PSII. Such unconnected LHCII most probably form the aggregation, which would not be visualized in our measurement condition because of the energy-dissipative state of LHCII aggregation^{5,60,61}. Thus, the observed structural dynamics might reflect the changes in Chl fluorescence lifetime due to the interaction between PSII-LHCII supercomplex and LHCII aggregation. It is also possible that the free LHCII existing as a pool^{50,51} might be visualized, as it is migrating between the two photosystems during state transitions¹. The other explanation is that the distortion of thylakoid membrane structure due to the presence of lincomycin would simply be visualized.

In conclusion, our live cell imaging has visualized the structural flexibility of thylakoid membranes *in vivo*. Our observation provides evidence for the importance of structural stability of the entire thylakoid membrane network, while the membrane structure itself is structurally flexible. The significance of such structural flexibility to protein interaction and reorganization will be an issue to be answered next. The dynamic aspects of photoacclimation mechanisms in green algae and higher plants have recently been shown by biochemical analysis. This study will lead to the future live cell imaging to uncover more detailed information of the spatiotemporal dynamics of thylakoid membrane proteins regulating the photoacclimation mechanisms *in vivo*.

Methods

Strain and growth conditions. Wild-type *P. patens* (Gransden 2004) protonemata were grown on BCDATG agar media⁶² at 25°C under 20 μmol photons m⁻² s⁻¹. For confocal microscopy, the protonemata were grown on a glass-bottom dish with the agar media in similar conditions. To generate macrochloroplasts, the protonemata were grown on the agar contained 1 mM ampicillin for 5 to 7 days³². To inhibit chloroplast-encoded protein synthesis, the protonemata were grown on the agar contained 1 mM lincomycin for 5 to 7 days in similar conditions⁴¹.

Confocal microscopy and 3D deconvolution. We used a Zeiss LSM510 confocal laser scanning microscope with a ×63 Plan Apochromat 1.4 NA oil objective. An argon laser (488 nm, 10% laser power) and a 650 nm long-pass filter were used for observation with the image size of 512 × 512 pixel mode. The scan speed was 1.61 μs per pixel. The pinhole size was adjusted to 1.35 airy units for the better image acquisition and data processing. The gain was adjusted to obtain the optimal Chl fluorescence image. The optical serial sections were taken 5 slices with 0.2 μm intervals. For the time-lapse imaging, the 28 series of 3D image were acquired sequentially without the additional interval time, taking ~196 s in total, roughly ~7 s per each 3D image. The point spread function of the confocal microscope was measured by using the 0.1-μm TetraSpeck beads (Invitrogen). The measured point spread function was used for 3D deconvolution. Also, because each 3D image contains different time axes between Z-planes, we adjusted the fluorescence intensity of all pixels according to the correction of the difference in time axis between Z-planes (see Supplementary Note for details). With the data corrected the difference in time axis, the 3D reconstruction of deconvolution images was done by using the Velocity software (Improvision). The kymographs, the 3D surface plots, the sum images, and the extraction of Chl fluorescence signals for the dot-like and thread-like structures were performed by using ImageJ software (US National Institutes of Health). The average diameter of the dot-like structure was measured as full width at half maximum of the fluorescence intensity profile³⁵ obtained by using ImageJ software (Fig. S2).

- Eberhard, S., Finazzi, G. & Wollman, F. A. The dynamics of photosynthesis. *Annu. Rev. Genet.* **42**, 463–515 (2008).
- Li, Z., Wakao, S., Fischer, B. B. & Niyogi, K. K. Sensing and responding to excess light. *Annu. Rev. Plant Biol.* **60**, 239–260 (2009).
- Allen, J. F. & Forsberg, J. Molecular recognition in thylakoid structure and function. *Trends Plant Sci.* **6**, 317–326 (2001).
- Iwai, M., Takahashi, Y. & Minagawa, J. Molecular remodeling of photosystem II during state transitions in *Chlamydomonas reinhardtii*. *Plant Cell* **20**, 2177–2189 (2008).
- Iwai, M., Yokono, M., Inada, N. & Minagawa, J. Live-cell imaging of photosystem II antenna dissociation during state transitions. *Proc. Natl. Acad. Sci. USA* **107**, 2337–2342 (2010).
- Kouřil, R. *et al.* Structural characterization of a complex of photosystem I and light-harvesting complex II of *Arabidopsis thaliana*. *Biochemistry* **44**, 10935–10940 (2005).
- Kargul, J. *et al.* Light-harvesting complex II protein CP29 binds to photosystem I of *Chlamydomonas reinhardtii* under State 2 conditions. *FEBS J.* **272**, 4797–4806 (2005).
- Takahashi, H., Iwai, M., Takahashi, Y. & Minagawa, J. Identification of the mobile light-harvesting complex II polypeptides for state transitions in *Chlamydomonas reinhardtii*. *Proc. Natl. Acad. Sci. USA* **103**, 477–482 (2006).
- Telfer, A., Bottin, H., Barber, J. & Mathis, P. The effect of magnesium and phosphorylation of light-harvesting chlorophyll *a/b*-protein on the yield of P-700-photooxidation in pea chloroplasts. *Biochim. Biophys. Acta* **764**, 324–330 (1984).
- Delosme, R., Olive, J. & Wollman, F. A. Changes in light energy distribution upon state transitions: An *in vivo* photoacoustic study of the wild type and photosynthesis mutants from *Chlamydomonas reinhardtii*. *Biochim. Biophys. Acta* **1273**, 150–158 (1996).
- Vallon, O. *et al.* Lateral redistribution of cytochrome *b6/f* complexes along thylakoid membranes upon state transitions. *Proc. Natl. Acad. Sci. USA* **88**, 8262–8266 (1991).
- Finazzi, G. *et al.* Involvement of state transitions in the switch between linear and cyclic electron flow in *Chlamydomonas reinhardtii*. *EMBO Rep.* **3**, 280–285 (2002).
- Iwai, M. *et al.* Isolation of the elusive supercomplex that drives cyclic electron flow in photosynthesis. *Nature* **464**, 1210–1213 (2010).
- Peng, L., Fukao, Y., Fujiwara, M. & Shikanai, T. Multistep Assembly of Chloroplast NADH Dehydrogenase-Like Subcomplex A Requires Several Nucleus-Encoded Proteins, Including CRR41 and CRR42, in *Arabidopsis*. *Plant Cell* **24**, 202–214 (2012).
- de Bianchi, S., Dall'Osto, L., Tognon, G., Morosinotto, T. & Bassi, R. Minor antenna proteins CP24 and CP26 affect the interactions between photosystem II subunits and the electron transport rate in grana membranes of *Arabidopsis*. *Plant Cell* **20**, 1012–1028 (2008).
- Johnson, M. P. *et al.* Photoprotective energy dissipation involves the reorganization of photosystem II light-harvesting complexes in the grana membranes of spinach chloroplasts. *Plant Cell* **23**, 1468–1479 (2011).
- de Bianchi, S. *et al.* *Arabidopsis* mutants deleted in the light-harvesting protein Lhcb4 have a disrupted photosystem II macrostructure and are defective in photoprotection. *Plant Cell* **23**, 2659–2679 (2011).
- Tokutsu, R. & Minagawa, J. Energy-dissipative supercomplex of photosystem II associated with LHCSR3 in *Chlamydomonas reinhardtii*. *Proc. Natl. Acad. Sci. USA* **110**, 10016–10021 (2013).
- Goral, T. K. *et al.* Light-harvesting antenna composition controls the macrostructure and dynamics of thylakoid membranes in *Arabidopsis*. *Plant J.* **69**, 289–301 (2012).
- Aro, E. M. *et al.* Dynamics of photosystem II: a proteomic approach to thylakoid protein complexes. *J. Exp. Bot.* **56**, 347–356 (2005).
- Kato, Y., Sun, X., Zhang, L. & Sakamoto, W. Cooperative D1 degradation in the photosystem II repair mediated by chloroplastic proteases in *Arabidopsis*. *Plant Physiol.* **159**, 1428–1439 (2012).
- Gunning, B., Koenig, F. & Govindjee. A dedication to pioneers of research on chloroplast structure. *The Structure and Function of Plastids*, xxiii–xxxi (2007).
- Paolillo Jr, D. J. The three-dimensional arrangement of intergranal lamellae in chloroplasts. *J. Cell Sci.* **6**, 243–255 (1970).
- Wehrmeyer, W. Zur Klärung der strukturellen Variabilität der Chloroplastengrana des Spinats in Profil und Aufsicht. *Planta* **62**, 272–293 (1964).
- Brangeon, J. & Mustardy, L. Ontogenetic assembly of intra-chloroplastic lamellae viewed in 3-dimension. *Biol. Cell.* **36**, 71–80 (1979).
- Staehelein, L. A. Chloroplast structure and supramolecular organization of photosynthetic membranes. *Photosynthesis III: Photosynthetic Membranes and Light-Harvesting Systems* **19**, 1–84 (1986).
- Mustardy, L., Buttle, K., Steinbach, G. & Garab, G. The three-dimensional network of the thylakoid membranes in plants: quasihelical model of the granum-stroma assembly. *Plant Cell* **20**, 2552–2557 (2008).
- Austin 2nd, J. R. & Staehelein, L. A. Three-dimensional architecture of grana and stroma thylakoids of higher plants as determined by electron tomography. *Plant Physiol.* **155**, 1601–1611 (2011).
- Gunning, B. E. S. & Schwartz, O. M. Confocal microscopy of thylakoid autofluorescence in relation to origin of grana and phylogeny in the green algae. *Aust. J. Plant Physiol.* **26**, 695–708 (1999).
- Mehta, M., Sarafis, V. & Critchley, C. Thylakoid membrane architecture. *Aust. J. Plant Physiol.* **26**, 709–716 (1999).
- Abbe, E. Beiträge zur Theorie des Mikroskops und der mikroskopischen Wahrnehmung. *Archiv. Mikrosk. Anat.* **9**, 413–418 (1873).
- Kasten, B. & Reski, R. beta-lactam antibiotics inhibit chloroplast division in a moss (*Physcomitrella patens*) but not in tomato (*Lycopersicon esculentum*). *J. Plant Physiol.* **150**, 137–140 (1997).
- Machida, M. *et al.* Genes for the peptidoglycan synthesis pathway are essential for chloroplast division in moss. *Proc. Natl. Acad. Sci. USA* **103**, 6753–6758 (2006).
- Agard, D. A. & Sedat, J. W. Three-dimensional architecture of a polytene nucleus. *Nature* **302**, 676–681 (1983).
- Agard, D. A., Hiraoka, Y., Shaw, P. & Sedat, J. W. Fluorescence microscopy in three dimensions. *Method. Cell Biol.* **30**, 353–377 (1989).
- Herbstova, M., Tietz, S., Kinzel, C., Turkina, M. V. & Kirchhoff, H. Architectural switch in plant photosynthetic membranes induced by light stress. *Proc. Natl. Acad. Sci. USA* **109**, 20130–20135 (2012).



37. Barber, J. An explanation for the relationship between salt-induced thylakoid stacking and the chlorophyll fluorescence changes associated with changes in spillover of energy from photosystem II to photosystem I. *FEBS Lett.* **118**, 1–10 (1980).
38. Anderson, J. M. Consequences of spatial separation of photosystem-1 and photosystem-2 in thylakoid membranes of higher-plant chloroplasts. *FEBS Lett.* **124**, 1–10 (1981).
39. Trissl, H. W. & Wilhelm, C. Why do thylakoid membranes from higher plants form grana stacks? *Trends Biochem. Sci.* **18**, 415–419 (1993).
40. Chow, W. S., Kim, E. H., Horton, P. & Anderson, J. M. Grana stacking of thylakoid membranes in higher plant chloroplasts: the physicochemical forces at work and the functional consequences that ensue. *Photochem. Photobiol. Sci.* **4**, 1081–1090 (2005).
41. Belgio, E., Johnson, M. P., Juric, S. & Ruban, A. V. Higher plant photosystem II light-harvesting antenna, not the reaction center, determines the excited-state lifetime-both the maximum and the nonphotochemically quenched. *Biophys. J.* **102**, 2761–2771 (2012).
42. Nevo, R., Charuvi, D., Tsabari, O. & Reich, Z. Composition, architecture and dynamics of the photosynthetic apparatus in higher plants. *Plant J.* **70**, 157–176 (2012).
43. Szabo, M. *et al.* Structurally flexible macro-organization of the pigment-protein complexes of the diatom *Phaeodactylum tricornutum*. *Photosynth. Res.* **95**, 237–245 (2008).
44. Nagy, G. *et al.* Kinetics of structural reorganizations in multilamellar photosynthetic membranes monitored by small-angle neutron scattering. *Eur. Phys. J. E* **36**, 69 (2013).
45. Goral, T. K. *et al.* Visualizing the mobility and distribution of chlorophyll proteins in higher plant thylakoid membranes: effects of photoinhibition and protein phosphorylation. *Plant J.* **62**, 948–959 (2010).
46. Sznee, K. *et al.* Jumping mode atomic force microscopy on grana membranes from spinach. *J. Biol. Chem.* **286**, 39164–39171 (2011).
47. Janik, E. *et al.* Molecular architecture of plant thylakoids under physiological and light stress conditions: a study of lipid-light-harvesting complex II model membranes. *Plant Cell* **25**, 2155–2170 (2013).
48. Owens, T. G., Webb, S. P., Mets, L., Alberte, R. S. & Fleming, G. R. Antenna size dependence of fluorescence decay in the core antenna of photosystem I: estimates of charge separation and energy transfer rates. *Proc. Natl. Acad. Sci. USA* **84**, 1532–1536 (1987).
49. Veerman, J. *et al.* Functional heterogeneity of photosystem II in domain specific regions of the thylakoid membrane of spinach (*Spinacia oleracea L.*). *Biochemistry* **46**, 3443–3453 (2007).
50. Wientjes, E., van Amerongen, H. & Croce, R. Quantum yield of charge separation in photosystem II: functional effect of changes in the antenna size upon light acclimation. *J. Phys. Chem. B* **117**, 11200–11208 (2013).
51. Galka, P. *et al.* Functional analyses of the plant photosystem I-light-harvesting complex II supercomplex reveal that light-harvesting complex II loosely bound to photosystem II is a very efficient antenna for photosystem I in state II. *Plant Cell* **24**, 2963–2978 (2012).
52. Tikkanen, M. *et al.* Phosphorylation-dependent regulation of excitation energy distribution between the two photosystems in higher plants. *Biochim. Biophys. Acta* **1777**, 425–432 (2008).
53. Chuartzman, S. G. *et al.* Thylakoid membrane remodeling during state transitions in *Arabidopsis*. *Plant Cell* **20**, 1029–1039 (2008).
54. Cevc, G. & Richardsen, H. Lipid vesicles and membrane fusion. *Adv. Drug Deliver. Rev.* **38**, 207–232 (1999).
55. Nagy, G. *et al.* Reversible membrane reorganizations during photosynthesis *in vivo*: revealed by small-angle neutron scattering. *Biochem. J.* **436**, 225–230 (2011).
56. Posselt, D. *et al.* Small-angle neutron scattering study of the ultrastructure of chloroplast thylakoid membranes - periodicity and structural flexibility of the stroma lamellae. *Biochim. Biophys. Acta* **1817**, 1220–1228 (2012).
57. Albertsson, P. A. A quantitative model of the domain structure of the photosynthetic membrane. *Trends Plant Sci.* **6**, 349–354 (2001).
58. Kim, E. H. *et al.* The multiple roles of light-harvesting chlorophyll a/b-protein complexes define structure and optimize function of *Arabidopsis* chloroplasts: a study using two chlorophyll b-less mutants. *Biochim. Biophys. Acta* **1787**, 973–984 (2009).
59. Kirchoff, H. Molecular crowding and order in photosynthetic membranes. *Trends Plant Sci.* **13**, 201–207 (2008).
60. Miloslavina, Y. *et al.* Far-red fluorescence: a direct spectroscopic marker for LHClI oligomer formation in non-photochemical quenching. *FEBS Lett.* **582**, 3625–3631 (2008).
61. Holzwarth, A. R., Miloslavina, Y., Nilkens, M. & Jahns, P. Identification of two quenching sites active in the regulation of photosynthetic light-harvesting studied by time-resolved fluorescence. *Chem. Phys. Lett.* **483**, 262–267 (2009).
62. Nishiyama, T., Hiwatashi, Y., Sakakibara, I., Kato, M. & Hasebe, M. Tagged mutagenesis and gene-trap in the moss, *Physcomitrella patens* by shuttle mutagenesis. *DNA Res.* **7**, 9–17 (2000).

Acknowledgments

We thank Drs. Mitsuyasu Hasebe and Yuji Hiwatashi for providing the *P. patens* ecotype strain and the extensive technical advice for using the moss; Kaoru Kotoshiba and Hiroe Watanabe for support with sample preparation. This work was supported by JST PRESTO, JSPS KAKENHI Grant Numbers 21870047 and 23687008, and grants from RIKEN Center for Advanced Photonics, Extreme Photonics Research Project.

Author contributions

M.I. designed and performed research. M.I. and M.Y. analyzed data. A.N. contributed new analytical tool. M.I. prepared figures and wrote the paper. All authors reviewed and discussed the manuscript.

Additional information

Supplementary information accompanies this paper at <http://www.nature.com/scientificreports>

Competing financial interests: The authors declare no competing financial interests.

How to cite this article: Iwai, M., Yokono, M. & Nakano, A. Visualizing structural dynamics of thylakoid membranes. *Sci. Rep.* **4**, 3768; DOI:10.1038/srep03768 (2014).



This work is licensed under a Creative Commons Attribution-NonCommercial-NoDerivs 3.0 Unported License. To view a copy of this license, visit <http://creativecommons.org/licenses/by-nc-nd/3.0>